8. T. T. Tsong, *Rep. Prog. Phys.* **51**, 759 (1988); G. Ehrlich, *Surf. Sci.* **246**, 1 (1991); G. L. Kellogg, *Appl. Surf. Sci.* **87/88**, 353 (1995).
9. S. C. Wang and G. Ehrlich, *Surf. Sci.* **239**, 301 (1990).
10. K. Stolt, W. R. Graham, G. Ehrlich, *J. Chem. Phys.* **65**, 3206 (1976).
11. P. J. Feibelman, *Phys. Rev. Lett.* **58**, 2766 (1987).
12. D. W. Bassett, *J. Phys. C* **9**, 2491 (1976).
13. G. L. Kellogg, T. T. Tsong, P. Cowan, *Surf. Sci.* **70**, 485 (1978).
14. P. Hofmann *et al.*, *ibid.* **337**, 169 (1995).
15. M. Doering, J. Buisset, H.-P. Rust, B. G. Briner, A. M. Bradshaw, *Faraday Discuss. Chem. Soc.* **105**, 163 (1996).
16. Several movie sequences of STM images have been posted on our Web site (http://www.fhi-berlin.mpg.de/of/of.html) to provide a more detailed impression of the characteristics of CO diffusion.
17. Strictly speaking, this expression is only correct in a limited temperature range, because D_0 is also weakly temperature dependent. Details can be found in (*1*).
18. B. Poelsma, L. K. Verheij, G. Comsa, *Phys. Rev. Lett.* **49**, 1731 (1982); J. E. Reutt-Robey, D. J. Doren, Y. L. Chabal, S. B. Christman, *J. Chem. Phys.* **93**, 9113 (1990); L. R. Becerra, C. A. Klug, C. P. Slichter, J. H. Sinfelt, *J. Phys. Chem.* **97**, 12014 (1993).
19. A further test for such STM-induced artifacts is to decrease the barrier resistance until individual CO molecules can be manipulated with the probe tip. We found that this happened typically at $R < 2$ Mohm. A repulsive tip-adsorbate interaction was observed, in accordance with other reports on molecular manipulation (*24, 25*). Because all images of a time-lapse series are scanned in the same direction, repulsive interactions deplete the sampled area by shuffling the adsorbates to the edges of the scan window. Such an effect was never observed for the tunneling conditions (R = 0.5 to 1 Gohm) used in the diffusion experiments.
20. The fits take into account the fact that "looplike" hopping sequences that bring the adsorbates back to their original sites can be overlooked in the experiment because of the finite time delay between sequential images. This effect, which increases the fraction of adsorbates that apparently have not moved, is much more important for chain hopping than for monomer hopping.
21. D. A. Reed and G. Ehrlich, *J. Chem. Phys.* **64**, 4616 (1976).
22. B. N. J. Persson, *Chem. Phys. Lett.* **149**, 278 (1988); A. Grossmann, W. Erley, H. Ibach, *Phys. Rev. Lett.* **71**, 2078 (1993).
23. Longer CO chains were also found to be very mobile, but it is difficult to quantitatively determine their hopping rate because they tend to break up easily.
24. T. A. Jung, R. R. Schlittler, J. K. Gimzewski, H. Tang, C. Joachim, *Science* **271**, 181 (1996).
25. B. G. Briner, M. Doering, H.-P. Rust, A. M. Bradshaw, *Phys. Rev. Lett.* **78**, 1516 (1997).
26. We acknowledge helpful discussions with H. Conrad and R. Liebenow.

29 May 1997; accepted 8 August 1997

The Mechanism of a C–H Bond Activation Reaction in Room-Temperature Alkane Solution

Steven E. Bromberg, Haw Yang, Matthew C. Asplund, T. Lian,*
B. K. McNamara,† K. T. Kotz, J. S. Yeston, M. Wilkens,
H. Frei,‡ Robert G. Bergman,‡ C. B. Harris‡

Chemical reactions that break alkane carbon-hydrogen (C–H) bonds are normally carried out under conditions of high temperature and pressure because these bonds are extremely strong (~100 kilocalories per mole), but certain metal complexes can activate C–H bonds in alkane solution under the mild conditions of room temperature and pressure. Time-resolved infrared experiments probing the initial femtosecond dynamics through the nano- and microsecond kinetics to the final stable products have been used to generate a detailed picture of the C–H activation reaction. Structures of all of the intermediates involved in the reaction of $Tp^*Rh(CO)_2$ ($Tp^* = HB–Pz_3^*$, Pz^* = 3,5-dimethylpyrazolyl) in alkane solution have been identified and assigned, and energy barriers for each reaction step from solvation to formation of the final alkyl hydride product have been estimated from transient lifetimes.

Since the initial discovery that the strong C–H bonds in alkanes undergo oxidative addition to certain transition metal complexes, the quest to understand and utilize this "C–H activation" reaction (Fig. 1, A and B) has been the focus of intense research effort (*1*). Insights into the individual steps involved in metal-mediated C–H activation reactions have been obtained from spectroscopic techniques with microsecond time resolution, with the goal of identifying the reaction intermediates (*2, 3*). However, the extremely rapid reaction rate prevents these established methods from monitoring the earliest kinetics at room temperature and requires that the experiments be performed in the gas phase (*4*), in liquefied noble gases (*5*), or in low-temperature matrices (*2, 6*) to slow down the reaction.

In the gas phase, photolysis of $CpRh(CO)_2$ ($Cp = C_5H_5$) yields the highly reactive CpRhCO, which reacts with alkanes at rates close to the gas-kinetic values (Fig. 1A) (*4*). Low-temperature matrix work also showed the formation of CO-loss products (*2, 6*). In liquid krypton solution, the solvated complex Cp*Rh(CO)·Kr ($Cp^* = C_5Me_5$, Me = methyl) is the first species observed. The alkane must then displace Kr before the final activation step can take place (*5*). These experiments established that the first step involves loss of a CO ligand to generate a coordinatively unsaturated intermediate. It is difficult, however, to generalize the results to room-temperature neat alkane solution because of the extreme changes in reaction conditions. In contrast to earlier work, our goal has been to study the reaction under the most relevant conditions, room-temperature alkane solution. To accomplish this, and to overcome the reaction-rate measurement limitations inherent in microsecond spectroscopy, we used ultrafast spectroscopy with picosecond (*7*) and femtosecond (*8*) time resolution, which allows access to the inter- and intramolecular processes that take place on time scales faster than diffusion.

The relatively low quantum yield of ~1% (*9*) for activation in the $CpM(CO)_2$ (M = Rh, Ir) system made ultrafast infrared (IR) observation of the reactive intermediates in this reaction impossible (*10*). To better understand the origin of the low quantum yield, we recently investigated the ultraviolet-visible spectroscopy of a C–H activating complex (*7*). In cyclohexane and *n*-pentane, ~99% of the molecules were directly promoted to a nondissociative excited state. As a result, relaxation back to the ground state was a much more favorable process than CO loss.

Identification and subsequent understanding of the reaction intermediates are required to build a detailed picture of the overall bond-activation reaction. In our initial study of the photochemistry of C–H activation, we used ultrafast IR spectroscopy to monitor the reaction with $Tp^*Rh(CO)_2$ ($Tp^* = HB–Pz_3^*$, Pz^* = 3,5-dimethylpyrazolyl) (Fig. 1B), taking advantage of its relatively high quantum yield (~30%) for the formation of activated product (*11*). In cyclohexane, $Tp^*Rh(CO)_2$ shows peaks at 1981 and 2054 cm^{-1} due to the antisymmetric and symmetric stretching modes of the two CO ligands. Upon irradiation, the static Fourier transform IR (FTIR) spectrum exhibits only a decrease in the intensity of the parent peaks and the corresponding formation of the final C–H activated product at 2032 cm^{-1} [see figure 1 of (*8*)]. On the

---

S. E. Bromberg, H. Yang, M. C. Asplund, T. Lian, B. K. McNamara, K. T. Kotz, J. S. Yeston, M. Wilkens, R. G. Bergman, C. B. Harris, Department of Chemistry, University of California at Berkeley, and Chemical Sciences Division, Lawrence Berkeley National Laboratory, Berkeley, CA 94720, USA.
H. Frei, Laboratory of Chemical Biodynamics, M. S. Calvin Laboratory, Lawrence Berkeley National Laboratory, Berkeley, CA 94720, USA.

*Present address: Department of Chemistry, Emory University, Atlanta, GA 30322, USA.

†Present address: Pacific Northwest National Laboratory, Post Office Box 999, Richland, WA 99352, USA.

‡To whom correspondence should be addressed.

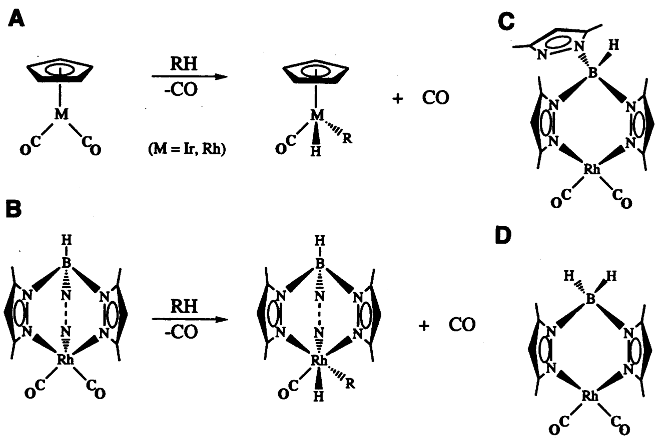

Fig. 1. The C–H activation reaction. **(A)** The overall reaction of CpM(CO)$_2$ (M = Rh, Ir). The quantum yield for this widely studied reaction is too low to observe the reactive intermediates. **(B)** The reaction of Tp*Rh(CO)$_2$. The larger quantum yield for this reaction allows detection of the intermediates. **(C)** Dechelated complex η^2-Tp*Rh(CO)$_2$. **(D)** Model system Bp*Rh(CO)$_2$. This molecule is stable in an η^2 configuration, similar to the proposed structure in (C).

picosecond time scale, two different monocarbonyl transient species were produced in the reaction in alkane solution. The CO absorption peak associated with the first intermediate was to the red of the 1981-cm^{-1} parent peak, whereas the second was shifted to the blue. In our earlier work, we reported that the energies of these peaks are 1972 and 1990 cm^{-1} in cyclohexane.

The first intermediate (heretofore denoted A) has a CO absorption at 1972 cm^{-1} and has been assigned to Tp*Rh(CO)·RH (RH = alkane solvent), a complex between the monocarbonyl and the solvent (*8*). The time scale for formation of the intermediate is consistent with those associated with solvent complex generation observed in previous studies of CpCo(CO)$_2$ (*12*), (acac)Rh(CO)$_2$ (acac = acetyl acetonate) (*10*), and M(CO)$_6$ (M = Cr, Mo, and W) (*13, 14*). After the CO dissociated from the metal center, the solvent moved in to occupy the empty site on the metal and formed a complex that vibrationally relaxed in 10 to 20 ps (*10*). The Tp*Rh(CO)$_2$ molecule shows similar reactivity and forms a new complex that vibrationally cools on a time scale of 23 ps (*8*). This monocarbonyl solvent complex then converts to the second intermediate, B, on a time scale of 200 ps.

The identity of B is more difficult to assign. There is some experimental and preliminary theoretical evidence to support the postulate that one of the pyrazolyl arms in the Tp*Rh(CO)·RH complex detaches from the metal center after photoexcitation (*2, 6*). In the Tp*Rh(CO)$_2$ starting material, the three pyrazolyl arms are coordinated to the Rh center to form an η^3 complex (Fig. 1B), whereas the dechelated complex would be η^2 (Fig. 1C) (*15*). In room-temperature solution, the Tp*Rh(CO)$_2$ complex exists as a mixture of η^3 and η^2 isomers, with equilibrium constant $K_{eq} = 100$ favoring the η^3 species (*16*). In addition, recent density functional theory calculations (*17*) indicate that the closely related monocarbonyl complex TpRhCO (Tp = HB–Pz$_3$, Pz = pyrazolyl) may be stable in an η^2-bound configuration. Static low-temperature matrix studies (*2, 6*) and ab initio calculations support the blue-shifted position of the CO stretch in η^2-Tp* complexes. Thus, the second intermediate observed in the ultrafast IR spectrum may be an η^2-Tp*RhCO·RH complex. Despite this support, there has been no experimental evidence for the involvement of an η^2 species in the early time dynamics of the C–H bond activation reaction at room temperature.

A model chemical system for probing the effect of dechelation on CO stretching frequencies and testing whether intermediate B is an η^2 solvent complex is Bp*Rh(CO)$_2$ (Bp* = H$_2$B–Pz$_2$*) (Fig. 1D) (*2, 6*). This complex, with only two pyrazolyl rings attached to the boron atom, is a known stable η^2 species. Because it has only two Rh-N bonds instead of three, the CO stretches of this compound are blue-shifted 30 wave numbers relative to the η^3-Tp*Rh(CO)$_2$ complex. Photoinduced loss of CO from Bp*Rh(CO)$_2$ should produce a monocarbonyl species whose coordination environment is similar to the proposed η^2-Tp*Rh(CO) intermediate. Briefly, the Bp*Rh(CO)$_2$ compound was prepared according to the literature (*18*) and dissolved in dry cyclohexane (~1.4 mM). The solution was sealed under a nitrogen atmosphere and flowed through a 1-mm IR cell. After irradiation at 295 nm, the spectrum was collected from 1960 to 2090 cm^{-1} at time delays of −10, 10, 66, 200, and 660 ps (*13*). The ultrafast IR spectra of Bp* in cyclohexane (Fig. 2) show that at 10 ps, the bleaching of the parent peaks at 2010 and 2080 cm^{-1} coincides with the growth of another peak at 1992 cm^{-1}. Thus, the spectrum of the η^2-Bp*RhCO matches that of the second intermediate in the Tp*Rh(CO)$_2$ system. There is, however, no peak at 1972 cm^{-1} as there is in the Tp*Rh(CO)$_2$ system, which suggests that the second intermediate in the reaction scheme is an η^2-Tp*RhCO·RH complex in which one of the Rh-N bonds is broken. With this proposed structure for the second intermediate, we have assigned all of the observable species in the ultrafast spectra and can focus on the bond-activation process.

In the Tp*Rh(CO)$_2$ system, the newly assigned second intermediate was stable to ~1 ns, the longest time we could measure with our ultrafast system, so we could not observe the formation of the final C–H activated product. In order to understand the complete reaction and establish whether other intermediates are involved, we must observe the final bond activation step and link this with the ultrafast dynamics. Previous studies with microsecond

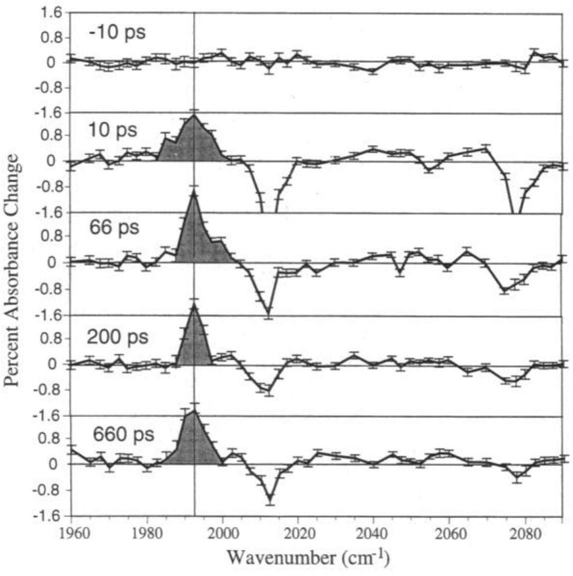

Fig. 2. Ultrafast transient IR spectra (irradiated at 295 nm) of Bp*Rh(CO)$_2$ in cyclohexane at room temperature. Time delays are given in each panel.

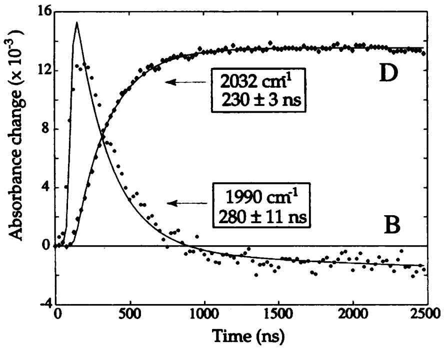

Fig. 3. Kinetic traces for transients formed upon the irradiation of Tp*Rh(CO)$_2$ in cyclohexane showing (curve B) the 1990-cm^{-1} transient (280 ns) and (curve D) the growth of the final product at 2032 cm^{-1} (230 ns).

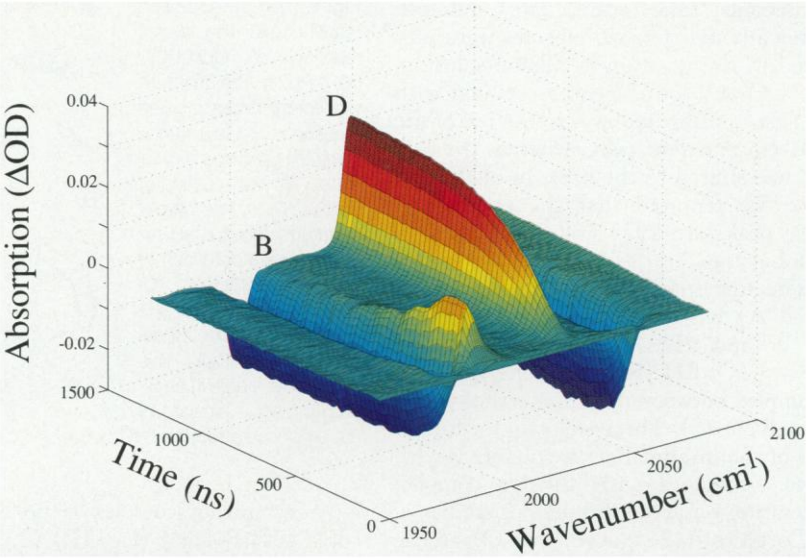

Fig. 4. Nanosecond transient change in absorption (ΔOD) of Tp*Rh(CO)$_2$ in cyclohexane after UV excitation. Note that the bleaches are constant throughout the spectrum, an intermediate is visible at 1990 cm^{-1}, and the growth of the final product appears at 2032 cm^{-1}.

time resolution showed that this step occurs in less than 1 μs (*19*), and so the time scale of the final bond-activating step is between 1 ns and 1 μs.

We then performed nanosecond IR experiments to probe C–H activation of Tp*Rh(CO)$_2$ in alkane solvents. The nanosecond FTIR system used in this study has been previously reported in detail (*20*). It consists of a pulsed Nd: yttrium-aluminum-garnet laser to initiate the photochemistry and a modified Bruker IFS88 Step-Scan FTIR spectrometer to record the transient absorptions. Samples in cyclohexane were excited at 355 nm, and their spectra were collected from 1600 to 2300 cm^{-1}. In the configuration used in this work, the spectrometer had a time resolution of ~50 ns and a frequency resolution of 4 cm^{-1}. The Tp*Rh(CO)$_2$ sample was prepared according to the literature (*21*) and stored under nitrogen. Solutions in each solvent were filtered, degassed, and sealed in an airtight flow cell. The flow rate was set to ensure that at a repetition rate of 10 Hz, each pulse encountered fresh sample. Ultraviolet (UV)-visible and IR spectra were collected throughout each run to monitor sample integrity. Solution concentrations were adjusted so that 80% of the excitation light was absorbed in the 1-mm path length of the IR cell. Similar procedures were followed for the Bp*Rh(CO)$_2$ sample.

Representative nanosecond time-resolved spectra of Tp*Rh(CO)$_2$ in cyclohexane (Fig. 3) show a decrease in C–O absorption at 1981 and 2054 cm^{-1}, due to the fast depletion of the parent molecule, and a new absorption at 1990 cm^{-1} that grew in in less than 50 ns. The observation of a single peak indicates that we are observing a monocarbonyl species, and the frequency of the peak matches the longest lived η^2-Tp*Rh(CO)·RH transient (curve B, Fig. 4) observed in the ultrafast IR measurements on this same system. The signal at 1990 cm^{-1} decayed to below the base line and could be fit to an exponential of ~280 ± 11 ns (curve B, Fig. 3). The subsequent formation of the alkyl hydride product was observed at 2032 cm^{-1} (curve D, Fig. 3). It grew with a single exponential time constant of 230 ± 3 ns. The decay time of intermediate B is longer than the formation time of the final product D because of thermal effects associated with the parent bleach at 1981 cm^{-1}. Temperature changes in the sample due to absorption of the laser pulse caused a time-dependent change in the refractive index of the sample (*22*). Such effects appear as time-dependent changes in absorbance near strong parent peaks and increase the observed lifetime of nanosecond transient intermediates. Because the transient at 1990 cm^{-1} was close to the parent bleach at 1981 cm^{-1}, it was strongly influenced by these effects, whereas the final product at 2032 cm^{-1} was further away from the bleaches and was not affected.

For the Bp*Rh(CO)$_2$ system, nuclear magnetic resonance (NMR) and IR studies showed that upon UV photolysis, there is no formation of C–H activated product, consistent with previous work (*11*). Time-resolved FTIR measurements showed only one peak at 1992 cm^{-1} due to the monocarbonyl solvent complex and no evidence for the formation of an alkyl hydride (Fig. 5). The solvent complex was stable for longer than 1 ms, but static FTIR spectra showed that it eventually recombined with CO or decomposed into unknown products. The inability of Bp*Rh(CO)$_2$ to activate C–H bonds suggests that not only is dechelation necessary to provide reactivity at the metal center, but rechelation is required to stabilize the product that results from the reaction.

The nanosecond time scale of the reaction indicates that there is a significant thermal barrier involved in the formation of the C–H activated product. Rate constants *k* determined from the experiments presented here allowed us to estimate values for the reaction barrier in room-temperature solutions. For the cyclohexane reaction, a simple treatment with transition-state theory and a rate constant of 4.3 × 10^6 s^{-1} [1/(~230 ns)] at 295 K gives the height of the free-energy barrier $\Delta G^{\ddagger}$ = ~8.3 kcal/mol (*23*). This estimate is comparable to the value of 7.2 kcal/mol calculated for the Cp*Rh(CO)$_2$ system by extrapolating the results of 183 K liquid

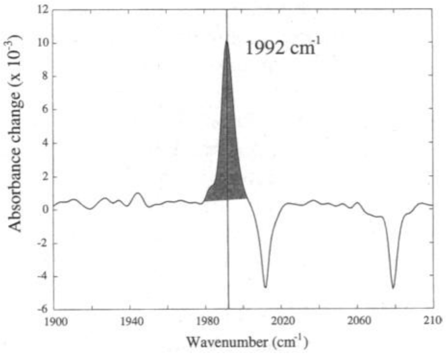

Fig. 5. Transient spectra obtained on irradiation of Bp*Rh(CO)$_2$ in cyclohexane 1 μs after photoexcitation showing the species observed at 1992 cm^{-1}.

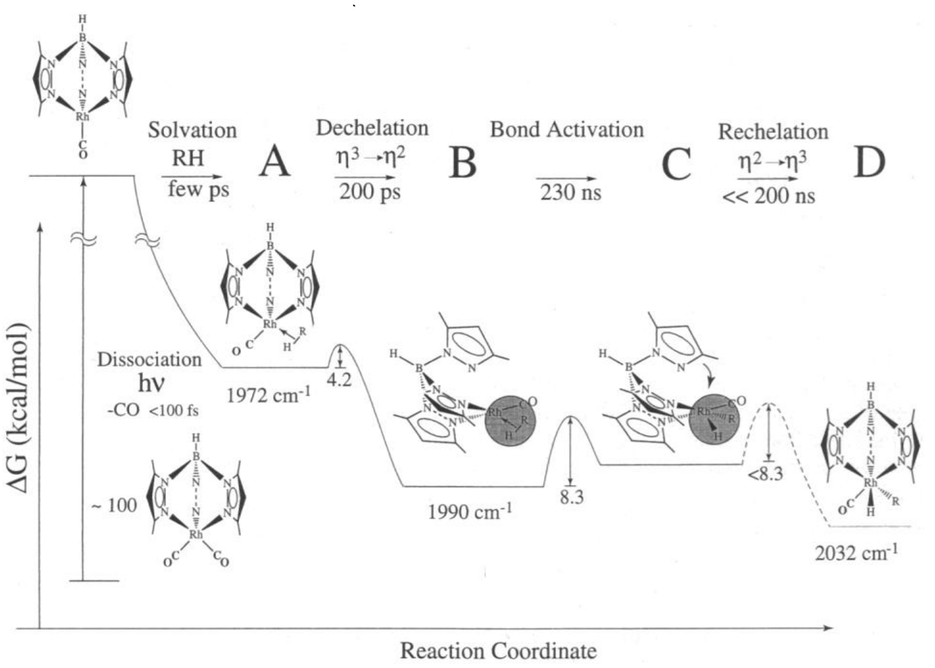

Fig. 6. Proposed mechanism and energy diagram for the C–H activation reaction of Tp*Rh$(CO)_2$ in alkane solution. These energy differences are estimates from separate ultrafast and nanosecond experiments. The stabilities of the intermediates are shown relative to each other and are not intended to be absolute.

Kr–cyclohexane experiments to room temperature (*24*).

We can combine these data with our earlier ultrafast result to assemble a comprehensive reaction coordinate diagram (Fig. 6). The rhodium dicarbonyl is initially in formal oxidation state I. Upon UV irradiation, the compound loses one CO in less than 100 fs (*25*) to form a vibrationally hot, coordinatively unsaturated (16-electron) complex, also in oxidation state I. The reactive species generated is quickly solvated in a barrierless reaction and then vibrationally cools in 20 ps (*12*, *26*). All subsequent processes that take place at the Rh center are thermal and do not depend on either the absorption of additional photons or residual photon energy in the complex. The CO stretching absorption of the first detectable solvated intermediate A could be observed at 1972 cm^{-1}, red-shifted from the lowest frequency peak of the parent complex at 1981 cm^{-1}.

Loss of one CO substantially reduces back-bonding from Rh and increases the electron density at the metal center. This change weakens the bonds between the Rh center and the σ-donating Tp* pyrazole ligands and eventually breaks a Rh-N bond. The complex traverses a 4.2 kcal/mol barrier [with $k = 5.0 \times 10^9$ s^{-1} or 1/(200 ps)] and forms the η^2-Tp* monocarbonyl complex B. Removal of the electrons formerly donated to the metal by the now detached arm of the Tp* ligand reduces the electron density at the metal again, shifting the CO absorption to higher frequency (1990 cm^{-1}). Detachment of the pyrazole ring in B increases the coordinative unsaturation of the solvate, making it more reactive toward C–H oxidative addition. The bond-breaking step occurs with a time constant of 230 ns, corresponding to a barrier of ~8.3 kcal/mol, and forms the unstable η^2 C-H activated complex C. This complex now has the metal center in formal oxidation state III, which reduces its electron density, providing the driving force for rechelation of the dangling pyrazole ring to form the final product, Tp*Rh(CO)(R)(H) (complex D).

Monitoring the C–H bond activation reaction in the nanosecond regime with IR detection has made it possible to establish directly the time scale for C–H bond-activation in room-temperature solution. The final breaking of the C–H bond occurs during the last step of the reaction, 230 ns after photolysis in cyclohexane. Before this bond can be broken, the Tp*Rh$(CO)_2$ complex must dissipate its initial excess vibrational energy and then break one of the Rh-N bonds. Immediately following the rate-limiting C–H bond-activation step, the Rh-N bond reforms to stabilize the final product. These steps before and after activation provide the structural and electronic environment around the metal center that allows the reaction to occur.

REFERENCES AND NOTES

1. A. H. Janowicz and R. G. Bergman, *J. Am. Chem. Soc.* **104**, 352 (1982); J. K. Hoyano and W. A. G. Graham, *ibid.*, p. 3723; R. G. Bergman, *Science* **223**, 902 (1984); B. A. Arndtsen, R. G. Bergman, T. A. Mobley, T. H. Peterson, *Acc. Chem. Res.* **28**, 154 (1995).
2. R. N. Perutz, S. T. Belt, A. McCamley, M. K. Whittlesey, *Pure Appl. Chem.* **62**, 1539 (1990).
3. R. N. Perutz, *ibid.*, p. 1103; *Chem. Ind.* **1991**, 462 (1991); *Chem. Soc. Rev.* **22**, 361 (1993).
4. E. P. Wasserman, C. B. Moore, R. G. Bergman, *Science* **255**, 315 (1992).
5. A. A. Bengali, R. H. Schultz, C. B. Moore, R. G. Bergman, *J. Am. Chem. Soc.* **116**, 9585 (1994); A. A. Bengali, R. G. Bergman, C. B. Moore, *ibid.* **117**, 3879 (1995).
6. P. E. Bloyce, J. Mascetti, A. J. Rest, *J. Organomet. Chem.* **444**, 223 (1993); F. Pradella, D. Rehorek, M. Scoponi, S. Sostero, O. Traverso, *ibid.* **453**, 283 (1993).
7. S. E. Bromberg, T. Q. Lian, R. G. Bergman, C. B. Harris, *J. Am. Chem. Soc.* **118**, 2069 (1996).
8. T. Lian, S. E. Bromberg, H. Yang, R. G. Bergman, C. B. Harris, *ibid.*, p. 3769.
9. D. P. Drolet and A. J. Lees, *ibid.* **114**, 4186 (1992).
10. T. P. Dougherty, W. T. Grubbs, E. J. Heilweil, *J. Phys. Chem.* **98**, 9396 (1994).
11. A. J. Lees and A. A. Purwoko, *Coord. Chem. Rev.* **132**, 155 (1994); A. A. Purwoko and A. J. Lees, *Inorg. Chem.* **35**, 675 (1996); A. A. Purwoko, S. D. Tibensky, A. J. Lees, *ibid.*, p. 7049.
12. T. P. Dougherty and E. J. Heilweil, *J. Chem. Phys.* **100**, 4006 (1994).
13. T. Lian, S. E. Bromberg, M. C. Asplund, H. Yang, C. B. Harris, *J. Phys. Chem.* **100**, 11994 (1996).
14. J. C. King, J. Z. Zhang, B. J. Schwartz, C. B. Harris, *J. Chem. Phys.* **99**, 7595 (1993); M. Lee and C. B. Harris, *J. Am. Chem. Soc.* **111**, 8963 (1989); S. C. Yu, X. Xu, R. Lingle Jr., J. B. Hopkins, *ibid.* **112**, 3668 (1990).
15. In multidentate organometallic systems such as Tp*Rh$(CO)_2$, the number of bonds between the ligand and metal is denoted by η.
16. A. A. Purwoko and A. J. Lees, *Inorg. Chem.* **34**, 424 (1995).
17. S. Zaric and M. B. Hall, personal communication.
18. F. Bonati, G. Mingetti, G. Banditelli, *J. Organomet. Chem.* **87**, 365 (1975).
19. S. T. Belt, F. W. Grevels, W. E. Klotzbucher, A. McCamley, R. N. Perutz, *J. Am. Chem. Soc.* **111**, 8373 (1989).
20. H. Sun and H. Frei, *J. Phys. Chem. B* **101**, 205 (1997).
21. S. Trofimenko, *J. Am. Chem. Soc.* **89**, 6288 (1967); S. May, P. Reinsalu, J. Powell, *Inorg. Chem.* **19**, 1582 (1980).
22. T. Yuzawa, C. Kato, M. W. George, H. Hamaguchi, *Appl. Spectrosc.* **48**, 684 (1994).
23. Using $k \approx 1/\tau = (k_b/\eta)\exp(\Delta G^{\ddagger}/RT)$, where k is the rate constant, τ is the time constant, k_b is the Boltzmann constant, $\Delta G^{\ddagger}$ is the free energy of activation, R is the gas constant, and T is temperature.
24. R. H. Schultz *et al.*, *J. Am. Chem. Soc.* **116**, 7369 (1994).
25. A. G. Joly and K. A. Nelson, *Chem. Phys.* **152**, 69 (1991); *J. Phys. Chem.* **93**, 2876 (1989).
26. M. W. George, T. P. Dougherty, E. J. Heilweil, *J. Phys. Chem.* **100**, 201 (1996); W. T. Grubbs, T. P. Dougherty, E. J. Heilweil, *Chem. Phys. Lett.* **227**, 480 (1994).

27. We thank C. B. Moore for use of the FTIR spectrometer in his laboratory. We are grateful for support of this work by NSF (C.B.H.), and we acknowledge equipment used under the Office of Basic Energy Sciences, Chemical Sciences Division, U.S. Department of Energy contract DE-AC03-76F00098 (R.G.B).

19 June 1997; accepted 29 August 1997